**General information of the article**

**Type of paper:** Article

**Title: Experimental Study on the Regulation Function of Slit Dam against Debris Flows**

**Authors:** Gordon G. D. Zhou [1&2], H. S. *Hu [1&2], D. Song [1&2], T. Zhao [3], and X. Q. Chen [1&2]

*1. Key Laboratory of Mountain Hazards and Earth Surface Process/Institute of Mountain Hazards and Environment, Chinese Academy of Sciences (CAS), Chengdu, China*

*2. University of Chinese Academy of Sciences, Beijing, China*

*3. State Key Laboratory of Hydraulics and Mountain River Engineering, College of Water Resources and Hydropower, Sichuan University, Chengdu 610065, Sichuan, China*

*Corresponding author

**Information of the authors**

**Corresponding author**: Mr H. S. Hu

Ph.D student

E-mail: huhongsen15@mails.ucas.edu.cn

**Co-author:** Dr Gordon G. D. Zhou

Professor

E-mail: gordon@imde.ac.cn

**Co-author:** Dr D. Song

Associate Professor

E-mail: drsong@imde.ac.cn

**Co-author:** Dr T. Zhao

Associate Professor

E-mail: zhaotao@scu.edu.cn

**Co-author:** Dr X. Q. Chen

Professor

E-mail: xqchen@imde.ac.cn

# Experimental Study on the Regulation Function of Slit Dam against Debris Flows

**Abstract:** Slit dams are open-type structures used to mitigate debris-flow hazards by constricting the flow and attenuating the kinetic energy. However, slit dams are often filled up as they are designed to impede debris volume instead of reducing kinetic energy of debris flows. To better understand the regulation function of slit dams against debris flows, physical model tests were carried out using a 7-m-long flume. The water content and relative post spacing were varied to discern their influence on the regulation function. Results reveal that the velocity attenuation and trapping efficiency is strongly controlled by water content and relative post spacing. Water content fundamentally reflects the degree of liquefaction (effetive grain-contact stress) and capacity of energy dissipation of debris flows. When water content < 26%, relative post spacing has a noticeable effect on velocity attenuation, trapping efficiency, and run-out distance. In contrast, when water content ≥ 26%, the influence relative post spacing is negligible. Furthermore, a new relationship between velocity attenuation and trapping efficiency for the design of slit dams is proposed to avoid the slit dam being easily filled up by sediments contained in debris flows.

**Keywords:** Slit dam; debris flows; regulation function; relative post spacing, water content

## 1. Introduction

Debris flows are geological phenomena that can be characterized by their high solid fraction and wide range of particle sizes (Cui 1999). Debris flows surge downslope at high velocities due to gravity (Cui *et al.* 2017a) and pose a major threat to local populations and infrastructure due to their long run-out distances (Zhang 1993; Scott *et al.* 2001; Ni *et al*. 2014; Zhou *et al*. 2016). To intercept these hazardous phenomena, structural countermeasures are commonly installed along the predicted flow paths to dissipate the kinetic energy and retain the debris volume (Baldwin *et al.* 1987; Hübl *et al.* 2005; Cui *et al*. 2018). Closed-type dam, a retention structure, is typically used to store torrent sediments and to diminish energy (Jaeggi *et al.* 1997; Sodnik *et al.* 2015). However, closed-type dams are easily filled up because of their nonselective retention, and the permeability of closed-type dams would almost be lost once their drainage holes are blocked. Besides, if the closed-type dam is destructed, the stored torrent sediments may cause sediments-related disasters in amplified scales (Zhou *et al*. 2013) and affect the downstream infrastructures (White *et al*. 1997).

Open-type dams in particular are an attractive option when the service life of a retention structure is considered important (Heumader 2000; Ono *et al.* 2004; Mizuyama *et al.* 2008). On one hand, open-type dams have the same functions as closed-type dams: elevating the longitudinal profile of a torrent bed, stabilizing upstream hillslopes, reducing the erosive power of a flow, and reducing the total transported volume. On the other hand, some complementary functions are possible with the openings for the open-type dams (Piton et al. 2015; Piton 2016): filtering and storing the undesirable components during a flow event, regulating the peak flow by temporarily retaining water/sediment, and reducing the high-energy level of a debris flow to a lower level (energy dissipation). Choi *et al.* (2014a) reported that an array of baffles (belonging to open-type dam) can effectively diminish the energy of landslide flow by a series of flume experiments using dry uniform sand. Besides, the change of kinetic energy and discharge upstream and downstream baffles resulting from each baffle configuration was also examined by Discrete Element Method (Choi *et al.* 2014b; Law *et al.* 2015).

Slit dams, as one type of open-type dams, designed with one or several vertical opening(s) (Chanson 2004), are initially designed to retain large particles and weaken the peak discharge (Lien *et al.* 2000; Takahashi 2014; Choi *et al.* 2018). As to the design of a slit dam, relative post spacing ($b/d_{\max}$, $b$: post spacing, $d_{\max}$: maximum particle diameter) is the key parameter (Johnson and McCuen 1989; Lien *et al.* 2003), which will directly affect the trapping or regulation function of a slit dam. Mizuyama *et al.* (1988) and MLR (2004) recommended that $b/d_{\max}$ should be between 1.5 and 2.0 for design of slit dams. However, the field investigation (Shima *et al*. 2016) showed that a slit dam is more likely to be filledup with narrower relative post spacing ($b/d_{\max}\approx 1.5$) by granular materials contained in debris flow, causing the trapping capacity of a slit dam to be lost (Fig.1a and Fig.1b).

In fact, previous studies have reported the blockage condition of slit dams. Specifically, experimental results from Lin *et al.* (1988) revealed that slit dams have notable effect on trapping debris materials when $b/d_{\max} \leq 1.7$. Furthermore, Han and Ou (2006) reported that when $b/d_{\max} < 1.5$, the slit dam was blocked. The results from both engineering practice and past experimental studies have shown that slit dam will be blocked with condition of $b/d_{\max} \leq 1.5 \sim 2.0$, and it will trap granular materials contained in debris flow until the trapping capacity is lost. The narrow relative post spacing ($b/d_{\max} = 1.5 \sim 2.0$) is recommended to retain the flow volume in the densely populated areas like Japan and Hong Kong, so that the infrastructures close to outlet of channels will not be damaged by debris flows.

This study focuses on the regulation function of a slit dam against debris flows. The interaction processes between debris flows and a slit dam, the attenuation of the kinematic energy (velocity), as well as the retention capacity of the debris materials were investigated to quantify the regulation function of slit dams.

# 2. Flume model tests

## 2.1 *Scaling*

Small-scale flume modeling were widely adopted to investigate the complex flow interaction between mass movement and structures (Choi *et al*. 2014a; Ng *et al*. 2015), The viscous effects may be quite significant at miniature scales while less significant at large scales and the dissipation of nonequilibrium pore water pressures occurs very rapidly compared with the duration of debris flow (Iverson *et al.* 2004; 2015). Despite this, since small-scale flume modelling can provide a controlled and systematic manner to study mechanisms of flow-structure interaction (Choi *et al*. 2015). Scaling is a powerful tool to design physical models to ensure that the test outcome is similar with that of the prototype (Iverson 1997; 2015). The Froude number (*Fr*) is widely adopted to characterize dynamic similarity in hydraulics (Heller 2011; Lobovský *et al.* 2014), channelized granular flows (Chehata *et al.* 2003; Hauksson *et al.* 2007), and geophysical flows (Hübl *et al.* 2009; Choi *et al*. 2015). Both Hübl *et al.* (2009) and Armanini *et al.* (2011) demonstrated that the *Fr* is a key dimensionless parameter to scale debris flows impacting on structures. The *Fr* macroscopically quantifies the ratio of the inertial to gravitational forces. To correct the gravitational component of *Fr* by considering the inclination of the channel, *Fr* can be expressed as follows (Choi *et al.* 2015):

$$Fr = \frac{v}{\sqrt{gh\cos\theta}} \tag{1}$$

where $v$ is the frontal velocity, $g$ is the gravitational acceleration, $h$ is the maximum approaching flow depth (because the damage of structures usually appeared when debris flows approach with maximum flow depth), and $\theta$ is the inclination of the channel. Channelized debris flow have been reported to have characteristic *Fr* ranging from 0.45 to 7.56 based on field observations (Table 1) (McArdell *et al.* 2007; Hübl *et al.* 2009; Kwan *et al.* 2015). In this study, the dynamic similarity of debris flows is achieved by adopting *Fr* ranging from 1.65 to 6.96 that governs the dynamics behavior of debris flow during the interaction between debris flows and slit dams. It is acknowledged that the *Fr* numbers used in this study are bias towards large (1.65 to 6.96) compared with those obtained from majority natural debris-flow events (Table 1). Nevertheless, the *Fr* numbers used in our experiments are still in the range of that observed in field debris-flow events (0.45 ~ 7.56). Choi *et al*. (2015) have demonstrated that the higher *Fr* obtained in flume model tests is caused by the major limitation of small-scale experiments lying in limited initial volume. It leads to shallow flow depths and results in the flow velocity controlling *Fr* development of the flow. In this study, because of the fixed large inclination (30°), the subcritical Froude condition ($Fr < 1$) was not achieved.

### 2.2 *Model setup*

The experiments were carried out using a flume model with an overall length of 7.0 m, a channel width of 0.3 m, and depth of 0.35 m, respectively. The flume is located at the Dongchuan Debris Flow Observation and Research Station (DDFORS), in the Dongchuan District of Yunnan Province, China. Figure 2a shows the flume, which consists of a storage tank, a channel with two different inclinations, and a deposition section consisting of an unchannelized horizontal plate (2.5 m long and 1.5 m wide). The storage tank has dimensions of 1.0 m in length, 0.3 m in width, and 0.8 m in depth, with capacity of 0.15 $m^3$ when inclined at 30°. The debris mixture within the storage tank is retained using a gate, which is controlled manually. The inset in Fig. 2a shows a natural debris-flow sloping channel in Kangding county, Sichuan, China. Natural debris-flow channels typically consist of two angles. The upper part of channel with steeper angle is usually regarded as a transportation zone, and the lower part as deposition zone.

In the model tests, the upper section of the channel is inclined at 30° and has a length of 3.0 m. The downstream section is inclined at 7.6° and has a length of 4.0 m. To observe the run-out distance of the debris flow, the outlet of the flume was connected to the horizontal plate. The channel bed is made up by steel plate. The channel-bed roughness is characterised by interface friction angle between channel bed and granular used in the tests. It was measured in laboratory using the method reported by Savage and Hutter (1989). The interface friction angle was measured as 25.3°. A model of slit dam was installed at 2.8 m upstream of the intersection point between the outlet of the flume and the horizontal plate (Fig. 2b). The slit dam consists of three posts (Fig. 2c). The post spacing of the model slit dam varies from 27 mm to 72 mm by decreasing thickness of the posts.

### 2.3 *Instrumentation*

To measure the flow depth of debris flows, three laser sensors (Leuze, ODSL 30/V-30M-S12, named Lasers A to C) with resolution of 1 mm were mounted at the top of the channel at monitoring sections A, B, and C. Meanwhile, three cameras (SONY FDR-AX40, named camera A to C) with resolution of 1440×1080 pixels and frame rate of 25 frame per second (fps) were fixed over the channel and adjacent to the laser sensors to capture the kinematics of the test. Three grid lines, at interval of 0.01 m, were drawn at the base of the channel at sections A, B, and C to approximate the frontal velocity of the flow using the high-speed cameras. The velocity of the debris flow front is quite disintegrated after interacting with the slit dam, so the Section C locates at 2.8 m downstream of the slit dam, where the flow regime returns steady after interaction with slit dam.

In addition, a fourth camera (Nikon D 610, named camera D), with a resolution of 1280×720 pixels and frame rate of 60 fps, was positioned at the side of the flume to capture the interaction process between debris flow and slit dam. One differential strain-gauge pore pressure transducer (PPT, model KPSI 735, 0 ~ 18 kPa) was used to record the variation in pore water pressure of debris flow. Diaphragm of the transducer was separated from passing debris flow by a two-way hollow cylinder with water filled (Iverson *et al.* 2010). The top of cylinder was covered by a steel mesh filter to prevent the debris into the hollow cylinder (See Fig. 2d).

The degree of liquefaction, which is defined as the ratio of pore water pressure ($\sigma_w$) to the total normal stress of debris flow ($\sigma_t$), is used to represent the normalized influence of basal pore pressure on Coulomb resistance (Iverson *et al.* 2010). In this study, the total normal stress ($\sigma_t$) was estimated by the bulk density and approaching flow depth, that is $\sigma_t \approx \rho g h cos\theta$, where $g$ is the gravitational acceleration; and $\theta$ is the inclination of the channel (Iverson *et al.* 2010). Variation of the debris-flow parameters was recorded using a data loggers with a sampling rate of 20 Hz. In order to eliminate the noise from the data loggers and external disturbances, the signals were denoised by wavelet analysis method (Cui *et al.* 2015).

## 2.4 *Experimental materials and program*

The granular material for the tests was obtained from the debris-flow deposition fan of the Jiangjia Ravine near DDFORS. The granular material with diameters larger than 20 mm were removed to make sure all particles flow smoothly in the flume (Cui *et al.* 2015). For particles lager than 0.25 mm, they were measured using a set of sieves. The fine content, particles passing the 0.25 mm sieve, was measured using a Malvern Mastersizer 2000, which is designed to measure the size of small particles or the distribution of different sizes within a sample, based on the laser diffraction principle and particle size distribution statistics (Malvern Instruments Ltd, 2007). Figure 3 shows the grain-size distribution of the granular material used for the tests. The maximum diameter ($d_{max}$) of the granular material is 20 mm and the median size ($d_{50}$) is 3.6 mm. The bulk density of granular material was measured as 2680 kg/m$^3$ in the laboratory, and the void ratio is 0.6.

In this study, the water content of the debris flow, defined as the ratio of mass of water to the mass of granular material, and the relative post spacing were varied to discern their influence on the flow-dam interaction. Six groups of tests were conducted with using different water content and relative post spacing. The range of water contents was selected in the experiments based on trial and error. When the water content of debris flow is less than 18% (15% adopted), the granular-water mixture is not saturated. Besides, the velocity of the flow is very slow and the debris stops upslope of the slit dam. On the other hand, when the water content of debris flow is greater than 38% (40%

adopted), the *Fr* of approaching flow is higher than 8.5, which exceeds the common *Fr* range of natural debris flows. Therefore, the water content is varied from 18% to 38% with an interval of 4% in this study, modelling debris flows with different densities (*i.e.*, varying from 2160 kg/m$^3$ to 1830 kg/m$^3$; solid concentration varying from 0.69 to 0.50, respectively). The narrow relative post spacings $b/d_{max} < 2.0$ (*i.e.*, $b/d_{max}$ = 1.4 and 1.8) are used to check the retention function of a slit dam. The range of the relative post spacing $b/d_{max}$ varying from 2.3, 2.7, 3.1, and 3.6 were adopted to study the regulation function of a slit dam against debris flows. Prior to the slit-dam tests, reference tests marked with R were carried out to characterize the flow dynamics. Details of the modeling tests were summarized in Table 2.

### 2.5 *Testing procedures*

A series of reference tests (R-W18, R-W22, R-W26, R-W30, R-W34, and R-W38) without slit dam were first carried out, which were regarded as a reference to evaluate the regulation function of the slit dam in the slit-dam tests. During the reference tests, the frontal velocity and flow depth of the surge debris flow were recorded in Section A, B, and C.

After the tests, granular-water mixtures deposited upstream the position where to install the model slit dam were collected and weighed, which is used to remove the influence of the deposition effect during the debris flow traveling in the channel without slit dam (Choi *et al.* 2018). In the slit-dam tests, the interaction processes between debris flows and slit dam were recorded. The granular-water mixtures trapped by slit dam were collected and weighed when the fluid phases stopped segregating from granular-water mixture.

In all tests, the granular-water mixtures were continuously stirred to prevent consolidation before opening the gate. The base of channel was kept wet prior to the release of sediments in each tests in order to model the wet ground. After the gate was pulled-up vertically within about one second to ensure it be opened as rapid as possible, the data logger was triggered and measurements were obtained simultaneously. The speed of gate opening makes little difference on the experimental results, because the deviation of the approaching velocity is about 2% ~ 11% in each group of tests. The run-out distance, defined as the distance from the location where to install slit dam to the frontal head of the deposited debris flow, was also measured.

## 3. Results of reference tests

As shown in Fig. 4a, the velocity measured in Section A increases with the water content from 18% to 38% in the reference tests without slit dam. The velocity measured in Section C is higher than that measured in Section A. Especially, for the test with 18% water content, the debris flow did not reach section C, so the velocity measured in section B is adopted. The deposition rate is defined as the ratio of the deposited mass of granular-water mixtures located upstream the location where to install slit dam, including the material left in the storage tank, to the total mass of initial granular-water mixtures, which is used to characterize the deposition effect of the debris flow during its traveling (Fig. 4b). It is revealed that the deposition rate is about 40% in the test with water content 18%. While in the test with 38% water content, the deposition rate is about 4%. Figure 4c shows that the run-out distance also increases with increasing water content. Relationship between the degree of liquefaction and water content is also shown (Fig. 4d), and more details will be discussed later.

## 4. Observed interaction process between debris flow and slit dam

In this section, the retention and regulation function of a slit dam against debris flows is investigated. The interaction process between debris flows with different water content and slit dams with different relative post spacing is also examined (Table 2). Two typical water contents (*i.e.*, $W$ = 18% and 30%) and two typical relative post spacings (*i.e.*, $b/d_{max}$ = 1.4 and = 3.1) are chosen to illustrate the interaction process.

### 4.1 *Test with low water content and narrow relative post spacing*

Debris flow with low water content (low $Fr$ condition) approaches the slit dam with narrow relative post spacing. Taking the test S-W18-1.4 for an example, a thin and wedge-shaped debris flow front approaches slit dam at $t$ = 0 s (Fig. 5a) and impacts on the slit dam at $t$ = 0.22 s. The measured frontal velocity is 1.45 m/s (Fig. 5b). When the front of the debris flow impacts the slit dam, few debris is observed to pass through the slit dam, majority of debris is retained. Sediments depositing behind the slit dam form a dead zone. Meanwhile, the flowing trajectory started to change and a thin layer of run-up develops before the slit dam at $t$ = 0.35 s (Figs. 5c&d). As the interaction progress continues, more debris pile up on top of the dead zone (Fig. 5e). Pile-up occurs until the sediments reach the highest point of the flow (Fig. 5f). Afterwards, the deposited mass begins to propagate upstream along the surface of dead zone (Fig. 5g). The deposits eventually reaches a static state at $t$ = 1.33 s (Fig. 5h).

### 4.2 *Test with low water content and wide relative post spacing*

Debris flow with low water content (low $Fr$ condition) approaches the slit dam with wide relative post spacing. Taking the test S-W18-3.1 for an example, the measured frontal velocity is 1.46 m/s before approaching to the slit dam (Figs. 6a&b). Similarly, run-up is observed (Figs. 6c&d), followed by pile-up (Fig. 6e) and then the upstream propagation of debris (Fig. 6f) before eventually reaching a static state (Fig. 6h). The relative post spacing is 1.3 times larger than that in Fig. 5. This feature enables much more debris to pass through the slits. With a larger slit spacing, upstream propagation of debris is less pronounced. Comparing Fig. 6 with Fig. 5, the water contents of debris flow are kept at 18%, with the $b/d_{max}$ increasing from 1.4 to 3.1. The interaction processes are almost identical, except that more debris passes through the slit dam in test S-W18-3.1 with a wider $b/d_{max}$.

### 4.3 *Test with high water content and narrow relative post spacing*

Debris flow with high water content (high $Fr$ condition) impacts the slit dam with narrow relative post spacing. Taking the test S-W30-1.4 for an example, a thinner debris flow front with a faster velocity of 3.5 m/s approaches the slit dam at $t$ = 0 s (Fig. 7a). Upon impacting the slit dam, part of debris flow, main the slurry, passes through the slit dam and develop distinct run-up along face of the slit dam (Figs. 7b&c). Overtopping is observed at $t$ = 0.26 s (Fig. 7c) and $t$ = 0.43 s (Fig. 7d). Run-up continues to overtop the slit dam and the run-up region becomes thicker (Fig. 7d). Meanwhile, rolling backwards occurs in the run-up region, where part of debris flow hits the posts of the slit dam and is bounced backward (Fig. 7d). The vertical jet begins to fall down towards the channel base (Fig. 7e). At $t$ = 0.93 s, more distinct falling towards the channel base is observed, and there is a bouncing phenomenon when the granular-water mixtures splatter against the channel base (Fig. 7f). Then the granular-water mixtures in upstream of the slit dam start to back flow and its depth increases (Fig. 7g). At last, the sediments are retained by slit dam, and slurry contained in the granular-water mixtures flows through the slit dam (Fig. 7h). After the interaction between debris flow and slit dam, 63% drop in velocity is observed from the approaching velocity 3.5 m/s to 1.3 m/s measured in Section C. Comparing Fig. 7 with Fig. 5, with the same $b/d_{max}$ = 1.35, the difference in interaction process is obvious. The phenomena of run-up, dead zone, pipe-up, and backflow occur during the interaction between debris flow with water content of 18% and slit dam. However, when the water content increases to 30%, the interaction processes include run-up, overtopping, rolling backwards, bouncing phenomenon after sediments splashing down to the base of the flume, backflow, and no formation of dead zone is observed.

### 4.4 *Test with high water content and wide relative post spacing*

Debris flow with high water content (high $Fr$ condition) impacts on the slit dam with wide relative post spacing. Taking the test S-W30-3.1 for an example, the measured frontal velocity of a thin debris flow was 3.9 m/s (Fig. 8a). The debris flow impacts the slit dam and more granular-water mixtures flow through the post spacing. Meanwhile, the run-up mechanism is developed (Fig. 8b). The run-up process continues along the face of slit dam, but its region is not distinctly thicker than that observed in test S-W30-1.4 (Figs. 8c&d). No apparent overtopping is observed. At $t = 0.67$ s, rolling backwards occurs (Fig. 8e), which leads to a bouncing phenomenon upstream the slit dam, and the debris flow in downstream of slit dam starts to fall down to the channel base (Fig. 8f). Then, the granular-water mixtures upstream of slit dam start to back flow (Fig. 8g). Finally, majority of sediments flow through the post spacing and a few is retained by the slit dam (Fig. 8h).

Comparing Fig. 8 with Fig. 6, the water contents are 18% and 30% and the relative post spacing is 3.1. The main interaction processes observed in Fig. 6 are run-up, formation of dead zone, pile-up, and backflow. However, in Fig. 8, when the debris flow impacts on the slit dam, the interaction process is violent with the granular-water mixtures flying through the slit dam. Small part of debris flow runs up along the posts of slit dam and then falls down to the base of the flume, causing a bouncing phenomenon (Fig. 8f).

Comparing Fig. 8 with Fig. 7, the water contents of debris flow are kept at 30% and the $b/d_{\max}$ also increases from 1.4 to 3.1. The differences in these two tests are obvious. In test S-30-1.4, apparent run-up, overtopping, backwater effect, and bouncing after the debris flow falling down to base of the flume are observed. In contrast, in test S-W30-3.1, due to the wider $b/d_{\max}$, more debris pass through the slit dam in a jet flow manner, and no overtopping phenomenon is observed. The run-up and bouncing phenomenon after the granular-water mixtures falling down occur, but they are not obvious compared with those in test S-W30-1.4.

## 5. Regulation function of slit dam against debris flows

In this section, three factors, namely, velocity attenuation, trapping efficiency, and run-out distance, are used to evaluate the regulation function of slit dam.

### 5.1 *Velocity attenuation*

In previous study, velocity attenuation is regarded as one of the significant functions of debris flow barriers (Choi, 2016). Moreover, the impact force is proportional to the velocity of debris flow (Hübl and Holzinger 2003; Scheidl *et al.* 2013; He *et al.* 2016). Thus, velocity attenuation implies the impact force of debris flow would reduce accordingly. It is noted that the velocities measured in Section C (or in Section B for debris flow with 18% water content) are lower than those measured in Section A (Fig. 9a). The velocity measured in Section C demonstrates a positive correlation with the increasing water content, which is consistent with the frontal velocity measured in Section A performed in the reference test (Fig. 4a).

In order to compare the trend of velocity attenuation with varying water content and $b/d_{\max}$, the relationship of rate of velocity attenuation $R$, water content, and relative post spacing $b/d_{\max}$ is plotted in Fig. 9b. The definition of rate of velocity attenuation $R$ is expressed as follows:

$$R=\frac{V_{\mathrm{Sec.A}}-V_{\mathrm{Sec.C}}}{V_{\mathrm{Sec.A}}}\times 100\% \qquad (2)$$

For tests with water content of 18%, the $V_{\mathrm{Sec.C}}$ is replaced by $V_{\mathrm{Sec.B}}$ in Equation (2), because the debris flows with 18% water content cannot reach the observation Section C.

The rate of velocity attenuation $R$ drops with water content in a decreasing rate (Fig. 9b). $W$ = 26% could be regarded as an inflection point of this trend. In the range $W$ < 26%, with $b/d_{\max}$ increasing from 1.4 to 3.6, rate of velocity attenuation $R$ could drop from 100% to 30%. Especially, for tests with $W$=18% and $b/d_{\max}$ less than or equal to 1.8, the rate of velocity attenuation $R$ is 100%. In this condition, slit dam fully stops debris flow, which is consistent with the previous finding with narrow relative post spacing ($b/d_{\max}$ = 1.5 ~ 2.0). In the range $W \geq$ 26%, regardless of the post spacing, the difference of rate of velocity attenuation is within 6% ~ 14%. On the other hand, results also reveal 2.3 as an inflection point for the relative post spacing of slit dam. In the range $b/d_{\max}$ < 2.3, within the water content considered in this study, rate of velocity attenuation $R$ drops from 100% to about 50%. In contrast, in the range $b/d_{\max} \geq$ 2.3, rate of velocity attenuation $R$ does not vary much, with a drop about 12% ~ 28%.

### 5.2 *Trapping efficiency*

Trapping the sediments contained in debris flows can release the risk of debris flows in blocking culverts and destroying downstream infrastructures. However, high trapping efficiency leads to countermeasure structures to be easily filled up and lose their designed regulation function. Therefore, it is imperative to ascertain a reasonable trapping efficiency when designing slit dams. In this study, trapping efficiency of slit dam is defined as the ratio between mass of granular-water mixtures trapped by the slit dam ($M$-$M_0$) and the mass that would pass without slit dam installed ($M_T$-$M_0$) and is expressed as follows (Choi, 2018):

$$T = \frac{M - M_0}{M_{\mathrm{T}} - M_0} \times 100\% \tag{3}$$

where $M$ is the mass of granular-water mixtures trapped by the slit dam, including the material left in the storage tank; $M_0$ is the mass of granular-water mixtures depositing on the base of flume, locating upstream of the position where to install slit dam in reference test (Fig. 4c); $M_T$ is the total mass of granular-water mixtures used in each test.

Figure 10 shows the relationship between trapping efficiency and varying water content and relative post spacing. When the water content is 18% and the relative post spacing is 1.4, the spacing of slit dam is blocked by debris flow as a result the trapping efficiency gets to 100%. On the other hand, when the water content is 38% and the relative post spacing is 3.6, no granular-water mixtures are retained except the natural deposition in the reference test without slit dam. Generally, trapping efficiency decreases in a decreasing rate with the water content. It is apparent that the water content (degree of liquefaction) strongly controls the debris through the slit structure. In the range $W < 26\%$, trapping efficiency $T$ drop drastically with varying relative post spacing. In contrast, in the range $W \geq 26\%$, the trapping efficiency approaches constant. With regards the effects of relative post spacing, as expected, higher $b/d_{\max}$ results in lower trapping efficiency $T$. Especially, in the range $b/d_{max} \geq 2.3$ and $W \geq 26\%$, less than 12% of debris was retained by the slit dam.

The trapping efficiency $T$ generally decreases with the increasing relative post spacing (Fig.10). Especially, for the debris flows $W \geqslant 26\%$, when $b/d_{max} < 2.3$, the decline of trapping efficiency $T$ is apparently faster than that with $b/d_{max} \geqslant 2.3$. It can be speculated that $b/d_{max} = 2.3$ is a threshold for the formation of stable granular arches. When $b/d_{max} < 2.3$, the big boulders at the front of debris flow clog the post spacing, which contributes to the formation of firm force chains behind the slit dam (Shima *et al.* 2016). As a result, the trapping efficiency $T$ is high (more than 20%). On the contrary, when $b/d_{max} \geqslant 2.3$, the contribution of big particles to the formation of stable force chains become negligible. Accordingly, the trapping efficiency $T$ is low (less than 12%).

### 5.3 *Change in run-out distance*

Impeding the mobility of debris flow is regarded as a factor to evaluate the regulation function of a slit dam in this study. Figure 11a shows the relationship between the run-out distance, $b/d_{max}$, and water content. In the reference tests with no slit dam, when the water content increases from 18% to 38%, the run-out distance increases from 2.23 m to 5.04 m. In the slit-dam tests, as expected, all the run-out distances are shorter than those in the corresponding reference tests. The shortest run-out distance occurs in the tests with $W = 18\%$ in each group tests. In this study, the rate of run-out distance reduction $S$ is defined as the ratio of the difference between the run-out distance ($L_0$) in the reference test and the run-out distance ($L$) in slit-dam tests over the run-out distance in the reference test ($L_0$):

$$S = \frac{L_0 - L}{L_0} \times 100\% \tag{4}$$

The influence of water content and $b/d_{max}$ on the rate of run-out distance reduction $S$ is shown in Fig. 11b. Similarly, the degree of liquefaction is also plotted to analyze its influence on the rate of run-out distance reduction $S$. The rate of reduction in the run-out distance decreases with the increasing water content. When the water content is kept at 18%, with the $b/d_{max}$ increasing from 1.4 to 3.6, rate of run-out distance reduction $S$ drops 71%. However, when $W = 22\%$, the drop in run-out distance reduction rate $S$ is 21%. Furthermore, $W \geq 26\%$, the maximum differences in rate of run-out distance reduction $S$ is only 13% ~ 15% with the $b/d_{max}$ increasing from 1.4 to 3.6. This implies that, with water content $W \geq 26\%$, post spacing has limited influence on the run-out distance reduction.

### **5.4** ***Implications of the state of liquefaction***

Based on the analysis of velocity attenuation, trapping efficiency, and change in the run-out distance of debris flow, water content $W$ and relative post spacing $b/d_{max}$ are two key variables influencing on the interaction process and regulation effects. Especially, the water content $W$ = 26% and the $b/d_{max}$ = 2.3 are two critical values. Hürlimann *et al.* (2015) demonstrated that water content strongly influences the run-out distance of debris flows by laboratory experiments. Numerical simulations from Cui *et al.* (2017b) showed that warer contained in granular material results in the change of basal effective stress. In fact, water content essentially reflects degree of liquefaction of debris flows. Both flume experiments (Iverson 1997, 2010) and field observation (McArdell *et al.* 2007; McCoy *et al.* 2010) suggested that the basual fluid water pressure (proportional to the degree of liquefaction) contributes the mobility of debris flow. In the present sutdy, when the water content $W = 26\%$, the degree of liquefaction of debris flow is 55% (Fig. 4e). To further reveal the mechanism, the degree of liquefaction is also plotted in Fig. 9b, Fig. 10, and Fig. 11b to analyze the influence of debris flows state.

With lower degree of liquefaction, the grain-contact effective stress dominates. Force chains are much easier to be formed and the internal shearing of solid grains is enhanced. From the energy point of view, energy dissipation efficiency of the grain-contact effective stress is much higher than the viscous stress of liquid phase. Accordingly, the debris flows approach the slit dam with a lower velocity. This explains why, when $W < 26\%$, the debris flow with a lower velocity impacts on the slit dam, no distinct overtoping is observed, and the regulation effects are obviously influenced by $b/d_{\max}$.

On the contrary, with high degree of liquefaction, the effective stress of debris flow decreases, and debris flows are more fluid-like. Thus the basal resistance becomes minor, leading to higher mobility of debris flow. Besides, the inertial force of the solids dominates during the movement, resulting in debris flow with a higher energy approaching to the slit dam. Accordingly, when $W \geqslant 26\%$, debris flow with a higher velocity impacts on slit dam. When the relative post spacing $b/d_{max}$ is narrow, the granular-water mixtures can run up and overtop the slit dam. That further explains why when water content $W \geq 26\%$, the influence of relative post spacing $b/d_{max}$ on the regulation effects is less obvious.

## 6. *Compromise between rate of velocity attenuation and trapping efficiency*

In this study, the experimental results show that there is a positive correlation between the rate of velocity attenuation $R$ and the trapping efficiency $T$ resulting from a slit dam (Fig. 12). When the rate of velocity attenuation is high, the trapping efficiency is also high. When the relative post spacing $b/d_{max}$ is narrow, a high rate of velocity attenuation means much of the flow kinetic energy is dissipated by the slit dam. However, the high trapping efficiency indicates that the slit dam can be easily filled up by the granular materials carried by debris flow. On the contrary, a larger $b/d_{max}$ leads to a lower rate of velocity attenuation and also a lower trapping efficiency $T$. Majority of the debris would surge downstream with highly destructive power.

There is a conflict between rate of velocity attenuation $R$ and trapping efficiency $T$ for slit dam to regulation debris flow, *i.e.*, reaching a compromise between appropriate discharge velocity and retention of debris volume Therefore, it is imperative to find a compromised relative post spacing $b/d_{max}$ for the design of slit dam to maintain its regulation function. A comparison of rate of velocity attenuation $R$ and trapping efficiency $T$ under different $b/d_{max}$ is shown in Fig. 12. When $W < 26\%$ and $b/d_{max} <$ 2.3, the rates of velocity attenuation range from 78% to 100%. Furthermore, a high trapping efficiency from 37% to 100% is also observed. Whereas, when $W \geqslant 26\%$ and $b/d_{max} \geq 2.3$, the rate of velocity attenuation $R$ varies from 25% to 53%, and the trapping efficiency just ranges from 0 to 12%.

Slit dams are characterized by trapping function and regulation function against debris flows. Accordingly, a new relationship between velocity attenuation and trapping efficiency for the design of slit dams is proposed. Slit dams can be mainly used to trap the debris volume if the infrastructures need to be protected close to the outlet of channels. In this scenario, the recommendation of $b/d_{max}$ for a slit dam depends on the characteristic of debris flows. For instance, when $b/d_{max} = 1.8$, trapping efficiency is about 100% for debris flow with $W = 18\%$. Besides, if the slit dams are mainly used to attenuate the kinematic energy (velocity) instead of trapping debris materials to prolong the service life. Based on the findings in this study, when $W \geq 26\%$, the slit dams are recommended to be constructed with a relative post spacing $2.3 \leq b/d_{max} \leq 3.6$, which can provide a velocity attenuation of 25% to 53% and a trapping efficiency within 12%. This can, to a large extent, protect a slit dam from being easily filled up by sediments.

## 7. *Conclusions*

A set of flume experiments were carried out to study the effects of varying the water content and relative post spacing on the regulation function of a slit dam. The key findings from this study can be drawn as:

1. The impact mechanisms of debris flow against slit dams are governed by the parameters of relative post spacing and the water content. More specifically,

when water content < 26%, a relative significant (more than 50%) amount of material is retained upstream and pile-up occurs during the interaction processes, regardless of the relative post spacing up to 3.1. When the water content ≥ 26% and the relative post spacing $b/d_{\max} \leq 2.3$ no significant accumulation of debris was observed. However, smaller post spacing leads to flow constriction and therefore overflow occurred. When the water content ≥ 26% and the relative post spacing $b/d_{\max} > 2.3$, neither accumulation of material nor flow constriction was observed.

2. The regulation effects of a slit dam can be characterized using velocity attenuation, trapping efficiency, and run-out distance. By varying the water content from 18% to 38% and relative post spacing from 1.4 to 3.6, the rate of velocity attenuation ranges from 25% to 100%, the rate of run-out distance reduction increases from 8% to 100%, and the trapping efficiency varies from 0 to 100%. The results indicate that properly designed slit dams can efficiently regulate debris flow to serve as a sustainable and low-maintenance structural countermeasure.
3. When water content $W < 26\%$, the relative post spacing has noticeable effects on rate of velocity attenuation, trapping efficiency, and rate of run-out distance reduction. However, when water content $W \geq 26\%$, the influence is negligible. This is because water content essentially reflects the degree of liquefaction (effective grain-contact stress) and capacity of energy dissipation of debris

flows due to the enhanced internal shearing of debris flow influenced by low water content. High degree of liquefaction leads to higher mobility with much kinetic energy approaching the slit dam, resulting in distinct overtopping, low velocity reduction ratio, and low trapping efficiency.

4. A new relationship between velocity attenuation and trapping efficiency for the design of slit dams is proposed aiming to prolong the service life. When $W \geq$ 26%, the slit dam is recommended with a relative post spacing between 2.3 and 3.6, which provides velocity attenuation of 25% to 53% with trapping efficiency from 0 to 12%.

The findings presented in this study are based on the type of debris flow from Jiangjia Ravine near the DDFORS and the given *Fr* conditions (1.65 to 6.96). They are closely related to the approaching *Fr* conditions and the relative post spacing. Therefore, the findings can be extrapolated to other types of geological settings which could provide the same approaching *Fr* conditions. As to the most adverse conditions (e.g. fully saturated; *Fr* ~ 10 or below 1.0), they are worthwhile to be further studied in future work.

By the field observation, it was found that big boulders can accumulate at the front of debris flows, and the boulders were even as large as the flow depth (Suwa 1988). Choi *et al*. (2018) studied the influence of boulders on the performance of slit-type barrier by flume mode tests. It was demonstrated that the presence of boulders leads to blockage of the slit-type barrier resulting in a greater reduction in the velocity of water-dominant debris flows. Besides, the presence of driftwood affecting the function of open-check dam has been also reported by Piton (2016) and Shima *et al.* (2016). Accordingly, in further study, it is worth to explore on the interactions between debris flows containing big boulders or driftwood and slit dam.

## *Acknowledgments*

The authors acknowledge the financial support from the National Natural Science Foundation of China (grant No. 11672318), the Youth Innovation Promotion Association, CAS, and the Chinese Academy of Sciences (CAS) Pioneer Hundred Talents Program. The financial support from research grant T22-603/15-N provided by the Research Grants Council of the Government of Hong Kong SAR, China is also greatly appreciated.

## *References*

Armanini A, Larcher, M, and Odorizzi, M (2011) Dynamic impact of a debris flow front against a vertical wall. In Proceedings of the 5th International Conference on Debris-Flow Hazards Mitigation: Mechanics, Prediction and Assessment, pp. 1041-1049 Padua, Italy

Baldwin JE, Donley HF, Howard TR (1987) On debris flow/avalanche mitigation and control, San Francisco Bay area, California. Reviews in Engineering Geology 7: 223-236

Chanson H (2004) Sabo check dams-mountain protection systems in Japan. Internal Journal of River Basin Management 2(4): 301-307

Chehata D, Zenit R, Wassgren CR. (2003) Dense granular flow around an immersed cylinder. Physics of Fluids (1994-present) 15(6): 1622-1631

Choi CE, Ng CWW, Song D, Kwan JHS, Shiu HYK, Ho KKS, Koo RCH (2014 a) Flume investigation of landslide debris–resisting baffles. Canadian Geotechnical Journal, 51(5): 540-553

Choi CE, Ng CWW, Law RP, Song D, Kwan JSH, Ho KKS (2014b) Computational investigation of baffle configuration on impedance of channelized debris flow. Canadian Geotechnical Journal, 52(2), 182-197

Choi CE, Ng CWW, Au-Yeung SCH, Goodwin G (2015). Froude scaling of landslide debris in flume modelling. Landslides, 12(6): 1197-1206

Choi CE, Goodwin G, Ng CWW, Chu HK, Kwan, JSH, Pun WK (2016) Coarse granular flow interaction with slit-structures. Géotechnique Letters, 6(4): 1-8

Choi SK, Lee JM, Kwon TH (2018) Effect of slit-type barrier on characteristics of water-dominant debris flows: small-scale physical modeling. Landslides,15(1), 111-122

Cui P (1999) Impact of debris flow on river channel in the upper reaches of the Yangtze River. International Journal of Sediment Research 14(2): 201–203

Cui P, Zeng C, Lei Y (2015) Experimental analysis on the impact force of viscous debris flow. Earth Surface Processes and Landforms, 40(12), 1644-1655

Cui YF, Zhou XJ, Guo CX (2017a) Experimental study on the moving characteristics of fine grains in wide grading unconsolidated soil under heavy rainfall. Journal of Mountain Science 14(3), 417-431

Cui Y, Chan D, Nouri A (2017b) Coupling of Solid Deformation and Pore Pressure for Undrained Deformation–a discrete Element Method Approach. International Journal for Numerical and Analytical Methods in Geomechanics 41(18): 1943-1961

Cui Y, Choi CE, Liu H, Ng CWW (2018) Effects of Particle Size of Monodispersed Granular Flows Impacting a Rigid Barrier. Natural Hazards 91(3): 1179-1201.

Han W, Ou G (2006) Efficiency of slit dam prevention against non-viscous debris flow. Wuhan University Journal of Natural Sciences 11(4): 865-869

Hauksson S, Pagliardi M, Barbolini M, Jóhannesson T (2007) Laboratory measurements of impact forces of supercritical granular flow against mast-like obstacles. Cold Regions Science and Technology 49(1): 54-63

Savage SB, Hutter K (1989) The motion of a finite mass of granular material down a rough incline. Journal of fluid mechanics, 199, 177-215

Heller V (2011) Scale effects in physical hydraulic engineering models. Journal of Hydraulic Research 49(3): 293-306

He S, Liu W, Li X (2016) Prediction of impact force of debris flows based on distribution and size of particles. Environmental Earth Sciences 75(4): 298

Heumader J (2000) Technical debris-flow countermeasures in Austria-a review. Proceedings, Second International Conference on Debris-Flow Hazards Mitigation: Mechanics Prediction, and Assessment. pp. 443-464. TaiPei, Taiwan: ASCE

Hübl J, Fiebiger G (2005) Debris-flow mitigation measures. In Debris-flow hazards and related phenomena. Springer Berlin Heidelberg, pp: 445-487

Hübl J, Holzinger G (2003) Development of design basis for crest open structures for debris flow management in torrents: miniaturized tests for the efficiency estimation of debris flow breakers. WLS Report

Hübl J, Suda J, Proske D (2009) Debris flow impact estimation. Proceedings of the 11th international symposium on water management and hydraulic engineering, pp. 1-4. Ohrid, Macedonia

Hürlimann M, McArdell BW, Rickli C (2015) Field and laboratory analysis of the runout characteristics of hillslope debris flows in Switzerland. Geomorphology, 232, 20-32

Iverson RM (1997) The physics of debris flows. Reviews of geophysics 34(3):244–296

Iverson RM, Logan M, Denlinger RP (2004) Granular avalanches across irregular three-dimensional terrain: 2. Experimental tests. Journal of Geophysical Research: Earth Surface, 109(F1)

Iverson RM, Logan M, LaHusen RG, Berti M (2010) The perfect debris flow? Aggregated results from 28 large-scale experiments. Journal of Geophysical Research: Earth Surface, 115(F3)

Iverson RM, George DL (2015) Modelling landslide liquefaction, mobility bifurcation and the dynamics of the 2014 Oso disaster. Géotechnique 66(3): 175-187

Jaeggi MNR, Pellandini S (1997) Torrent check dams as a control measure for debris flows. In Recent developments on debris flows. Springer, Berlin Heidelberg, pp: 186-207

Johnson PA, McCuen RH (1989) Slit dam design for debris flow mitigation. Journal of Hydraulic Engineering 115(9): 1293-1296

Kwan JSH, Koo RCH, Ng CWW (2015) Landslide mobility analysis for design of multiple debris-resisting barriers. Canadian Geotechnical Journal, 52(9), 1345-1359.

Law RPH, Choi CE, Ng CWW (2015) Discrete-element investigation of influence of granular debris flow baffles on rigid barrier impact. Canadian Geotechnical Journal, 53(1), 179-185

Lien HP, Tsai FW (2000) Debris flow control by using slit dams. International Journal of Sediment Research 15(4): 391-409

Lien HP (2003) Design of slit dams for controlling stony debris flows. International Journal of Sediment Research 18(1): 74-87

Lin YY, Jiang YZ (1988) Experimental study on the effectiveness of slit dam on debris flow. Journal of Chinese soil and water conservation 19 (1): 40-57 (in Chinese)

Lobovský L, Botia-Vera E, Castellana F, Mas-Soler, J, Souto-Iglesias, A (2014) Experimental investigation of dynamic pressure loads during dam break. Journal of Fluids and Structures 48: 407-434

Malvern Instruments Ltd (2007) MAN0384-1.0 Mastersizer 2000 User Manual.

Mizuyama T, Suzuki H，Oikaka Y, Morita A (1988) Experimental study on permeable sabo dam. Journal of Japan erosion control engineering society. 41 (2), PP. 21-25 (in Japanese)

Mizuyama T (2008) Structural countermeasures for debris flow disasters. International Journal of Erosion Control Engineering 1(2):38-43

MLR (Ministry of Land and Resources) (2004) Design standards for debris flow hazard mitigation measures (DZ/T0239-2004), Beijing, China: Chinese Geological Survey, Ministry of Land and Resources (in Chinese)

McArdell BW, Bartelt P, Kowalski J (2007) Field observations of basal forces and fluid pore pressure in a debris flow. Geophysical Research Letters, 34(7)

McCoy SW, Kean JW, Coe JA, Staley DM, Wasklewicz TA, Tucker GE (2010) Evolution of a natural debris flow: In situ measurements of flow dynamics, video imagery, and terrestrial laser scanning. Geology, 38(8), 735-738.

Ni H, Tang C, Zheng W (2014) An Overview of Formation Mechanism and Disaster Characteristics of Post-seismic Debris Flows Triggered by Subsequent Rainstorms in Wenchuan Earthquake Extremely Stricken Areas. Acta Geologica Sinica 88(4): 1310-1328

Ng CWW, Choi CE, Song D, Kwan JHS, Koo RCH, Shiu HYK, Ho KKS (2015) Physical modeling of baffles influence on landslide debris mobility. Landslides, 12(1), 1-18

Ono GI, Mizuyama T, Matsumura K (2004) Current practices in the design and evaluation of steel sabo facilities in Japan. Proceedings of the INTERPRAEVENT International Symposium. pp. VII: 243-264. Riva del Garda, Italy

Piton G, Recking A (2015) Design of sediment traps with open check dams. I: Hydraulic and deposition processes. Journal of Hydraulic Engineering, 142(2), 04015045

Piton, G. (2016) Sediment transport control by check dams and open check dams in Alpine torrents (Doctoral dissertation, Grenoble Alpes)

Scheidl C, Chiari M, Kaitna R, Müllegger, M, Krawtschuk, A, Zimmermann T, Proske, D (2013) Analysing debris-flow impact models, based on a small scale modelling approach. Surveys in Geophysics 34(1): 121-140

Scott KM, Macías JL, Naranjo JA (2001) Catastrophic debris flows transformed from landslides in volcanic terrains: mobility, hazard assessment, and mitigation strategies. US Geological Survey Professional Paper 1630: 1-59

Shima J, Moriyama H, Kokuryo H, Ishikawa N, and Mizuyama T (2016) Prevention and Mitigation of Debris Flow Hazards by Using Steel Open-Type Sabo Dams. International Journal of Erosion Control Engineering, 9(3): 135-144

Sodnik J, Martinčič M, Mikoš M (2015) Are Torrent Check-Dams Potential Debris-Flow Sources? In Engineering Geology for Society and Territory-Volume 2. Springer, Cham, pp: 485-488

Suwa H. (1988) Focusing mechanism of large boulders to a debris-flow front. PhD thesis, Tokyo University, Japan

Takahashi T (2014) Debris flow: mechanics, prediction and countermeasures. CRC press

White S, García-Ruiz J M, Martí C, Valero B, Errea MP, and Gomez-Villar, A (1997) The 1996 Biescas campsite disaster in the Central Spanish Pyrenees, and its temporal and spatial context. Hydrological Processes 11(14): 1797-1812

Zhang S (1993) A comprehensive approach to the observation and prevention of debris flows in China. Natural Hazards 7(1): 1-23

Zhou GGD, Cui P, Chen HY (2013) Experimental study on cascading landslide dam failures by upstream flows. Landslides 10(5): 633-643

Zhou GGD, Wright NG, Sun Q (2016) Experimental Study on the Mobility of Channelized Granular Mass Flow. Acta Geologica Sinica 90(3): 988-998

# List of figures

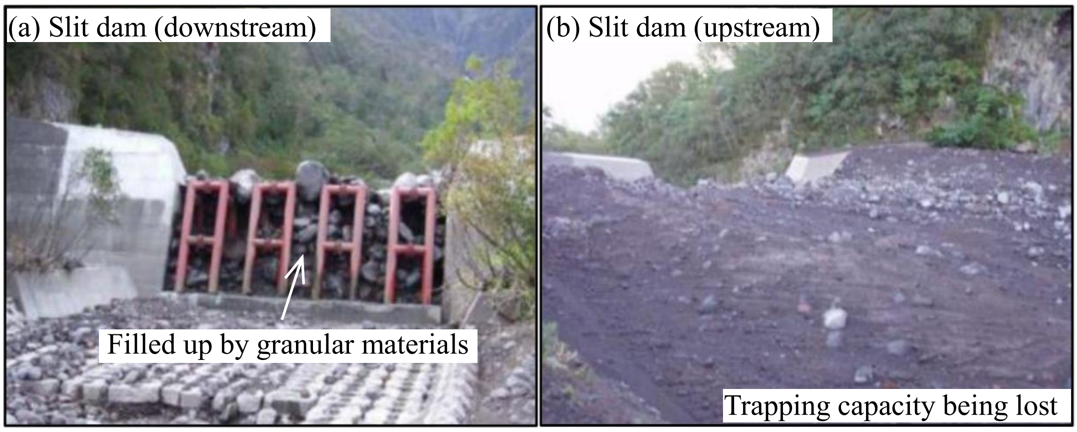


**Fig. 1** Slit dam filled up by granular materials from the downstream (a) and upstream (b) point of view (Shima *et al.* 2016).

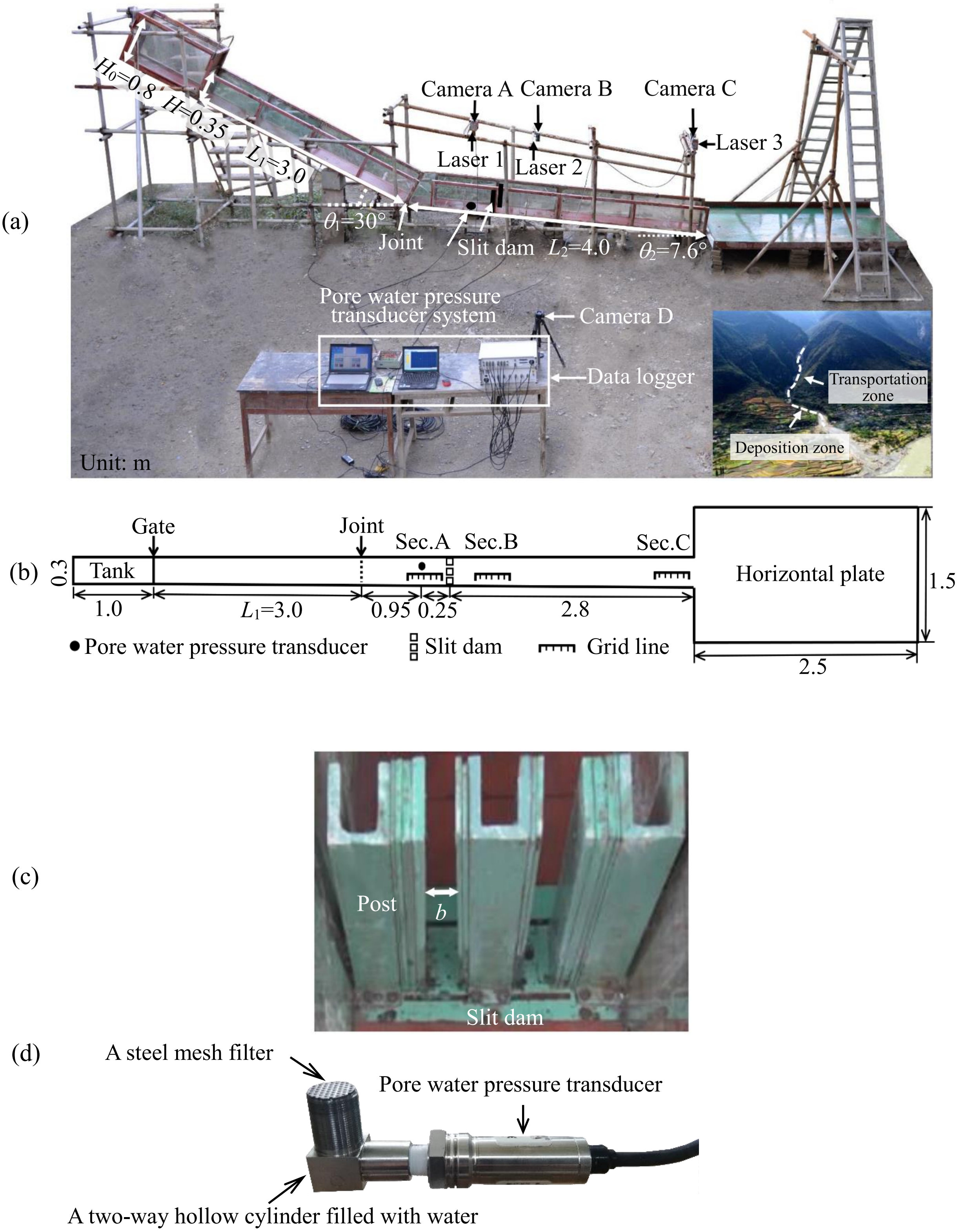


**Fig. 2** Setup of flume model tests. (a) side view of flume model; inset: a natural debris flow channel in Kangding county, Sichuan, China; (b) plan view of flume model; (c) model slit dam (all dimensions in m); and (d) the system of the pore water pressure sensor.

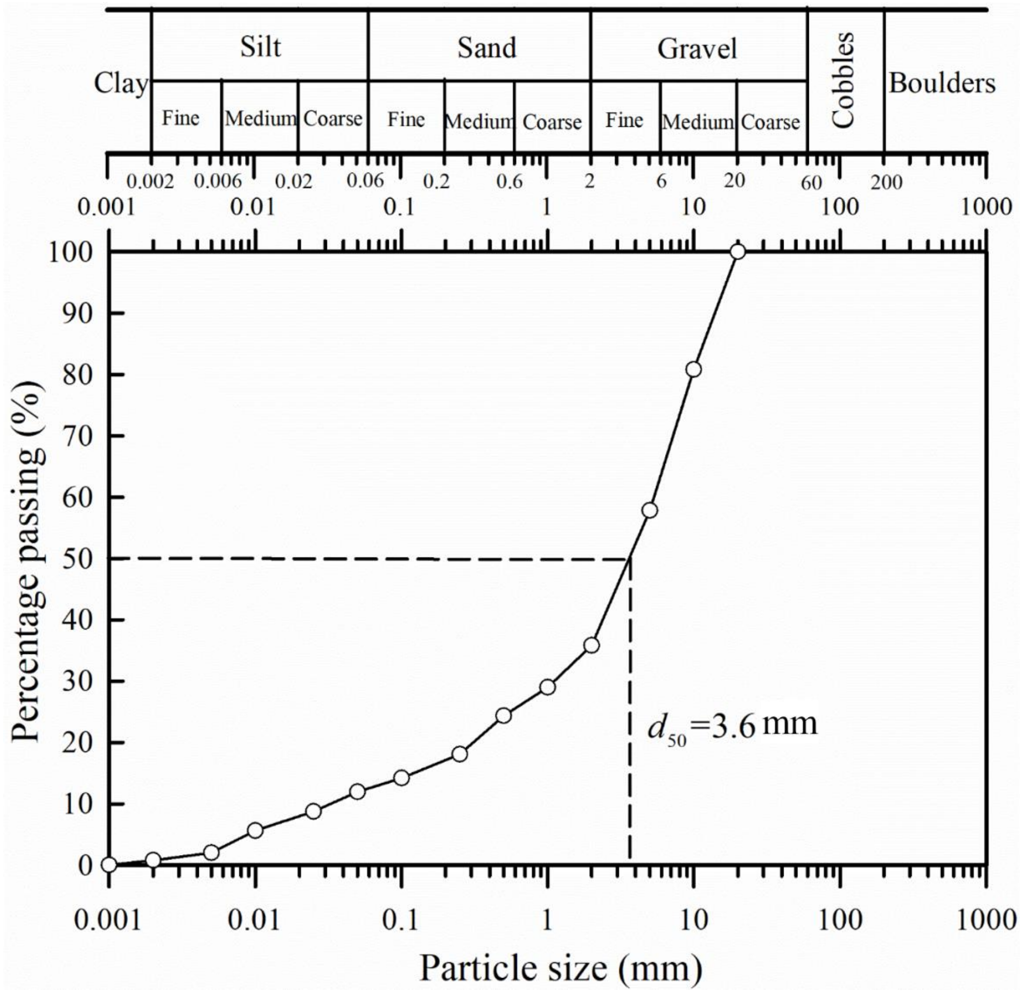


**Fig. 3** Particle size distribution of the granular material

(a)

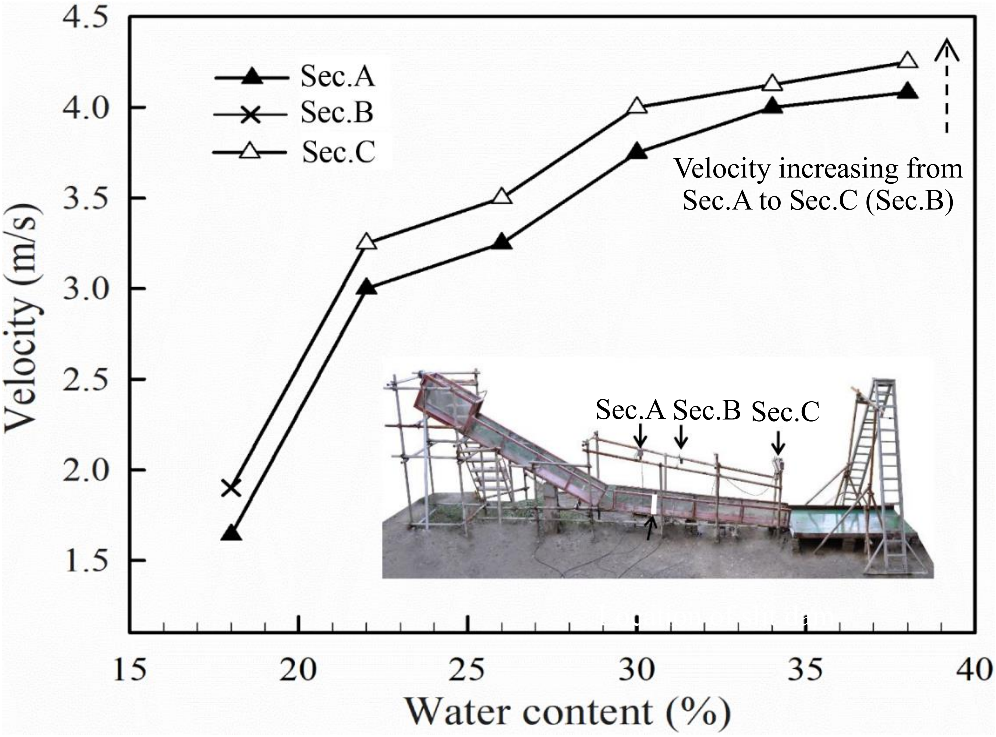

4.5
4.0
3.5
3.0
2.5
2.0
1.5
Velocity (m/s)
Sec.A
Sec.B
Sec.C
Velocity increasing from
Sec.A to Sec.C (Sec.B)
Sec.A
Sec.B
Sec.C
15
20
25
30
35
40
Water content (%)


(b)

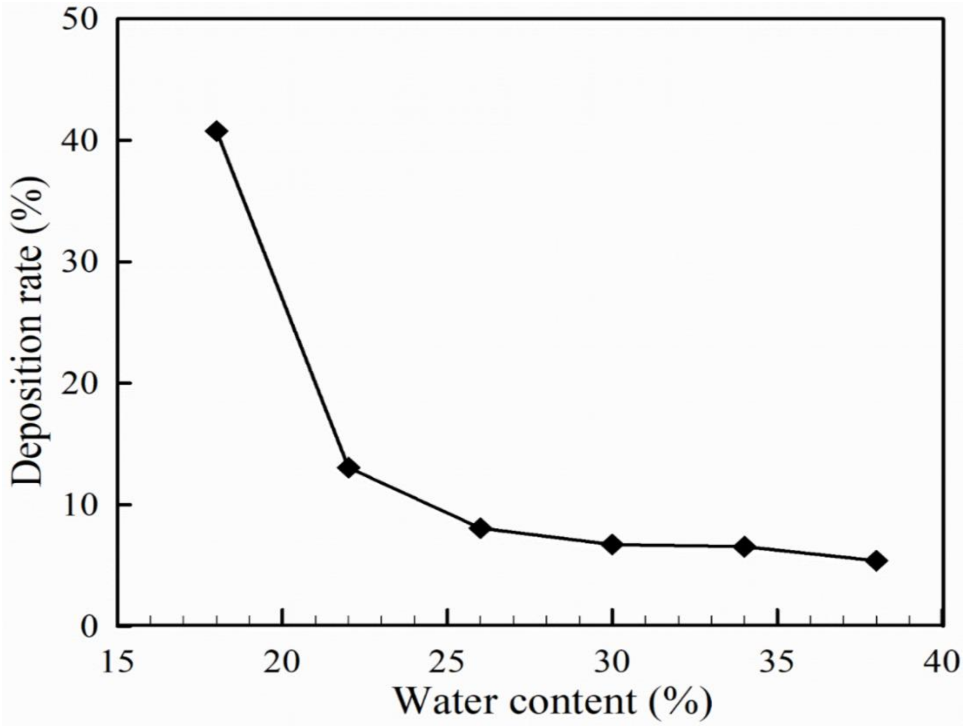

50
40
30
20
10
0
Deposition rate (%)
15
20
25
30
35
40
Water content (%)

(c)

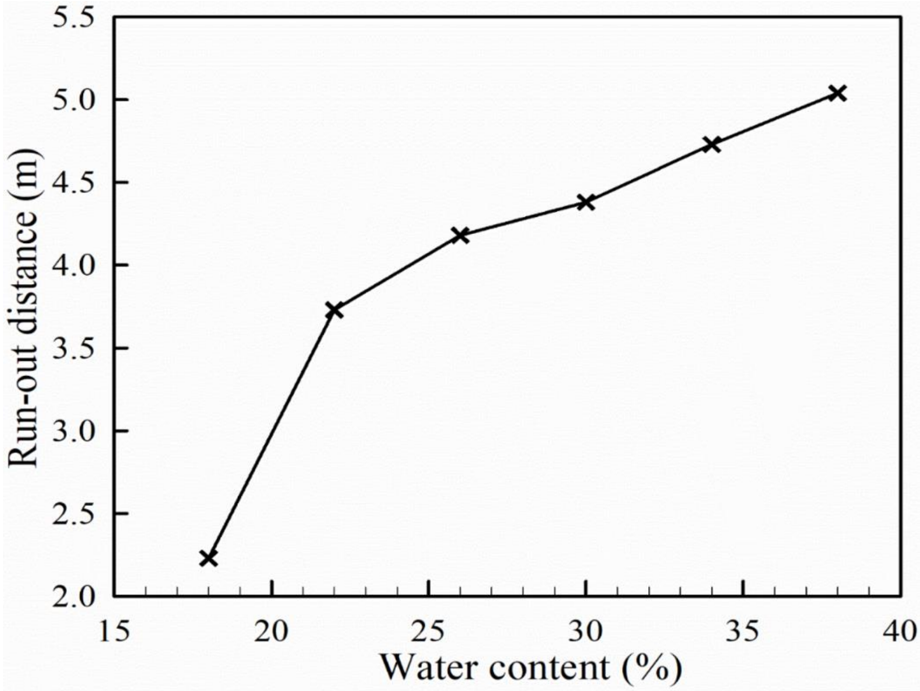


(d)

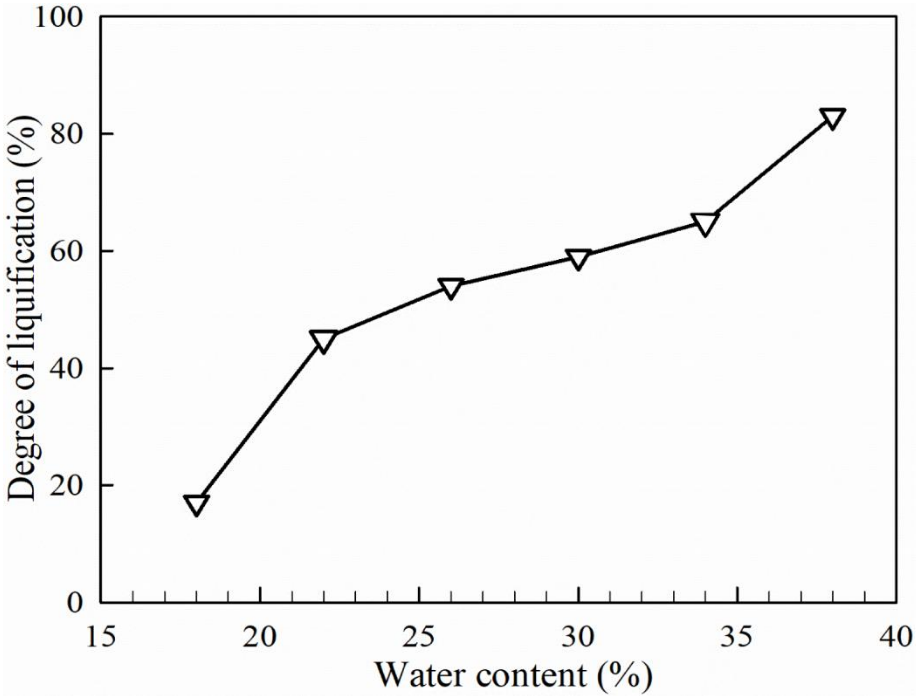


**Fig. 4** Relationship between water content and (a) approaching velocity in Section A, B (only for debris flow with *W*=18%) and C; (b) deposition rate; (c) run-out distance; and (d) degree of liquefaction in the reference tests.

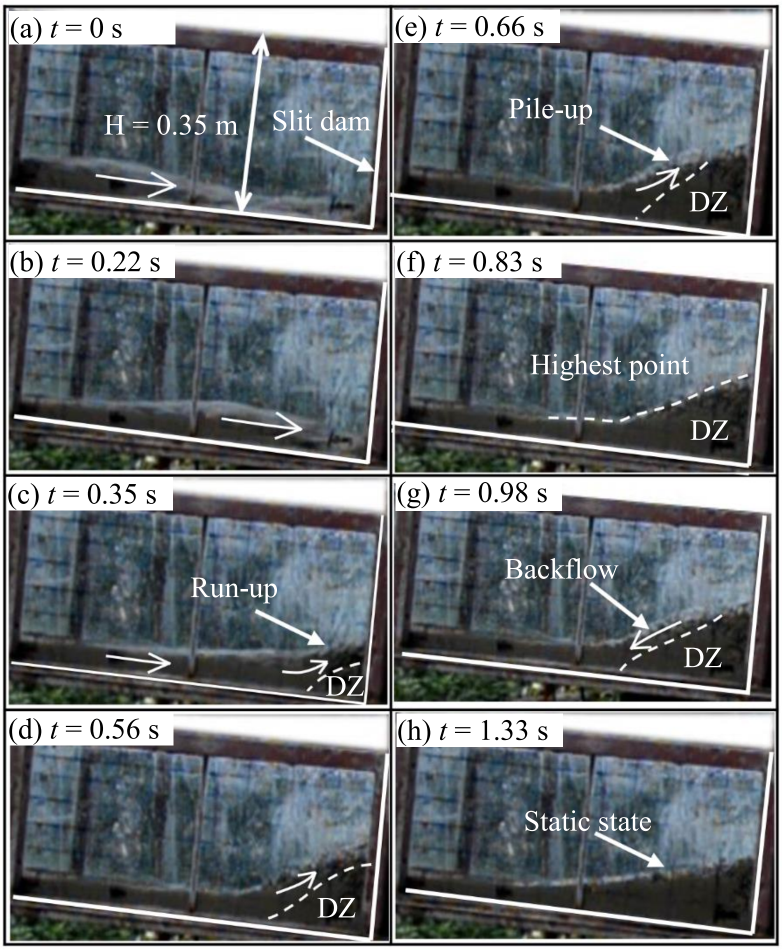


**Fig. 5** Interaction process between debris flow with low water content ($W$ = 18%) and slit dam with narrow relative post spacing ($b/d_{\max}$ = 1.4): test S-W18-1.4. DZ represents "dead zone".

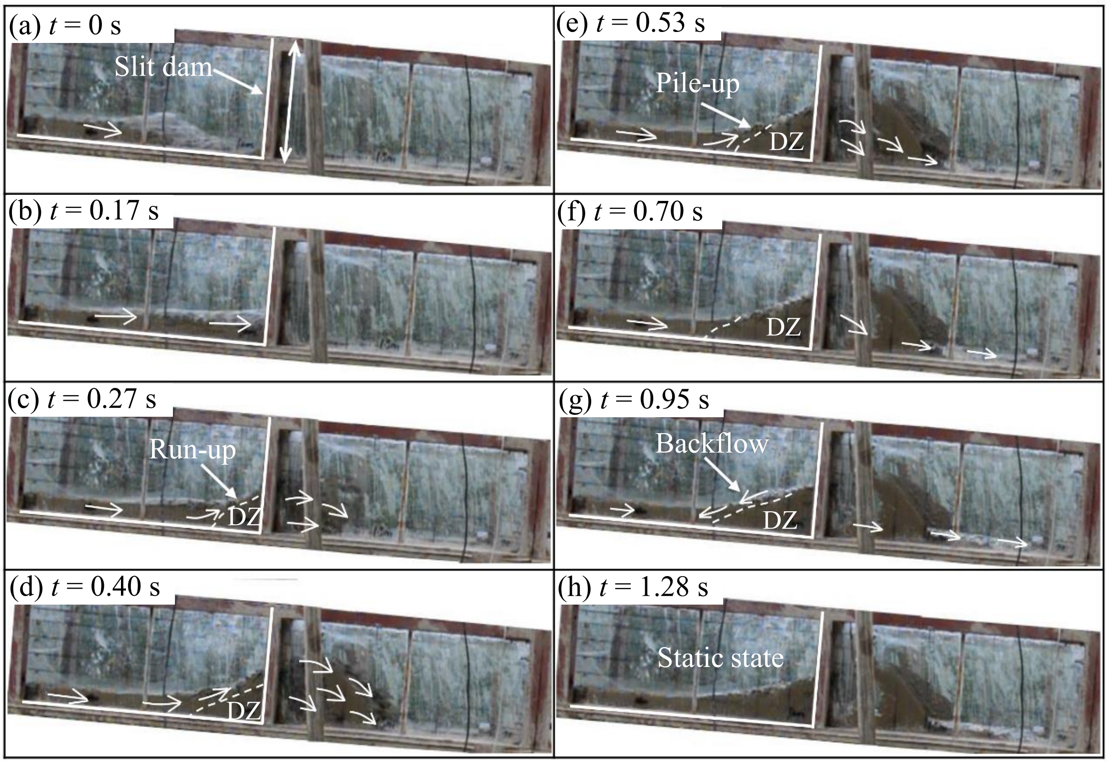


**Fig. 6** Interaction process between debris flow with low water content ($W$ = 18%) and slit dam with wide relative post spacing ($b/d_{\max}$ = 3.1): test S-W18-3.1. DZ represents "dead zone".

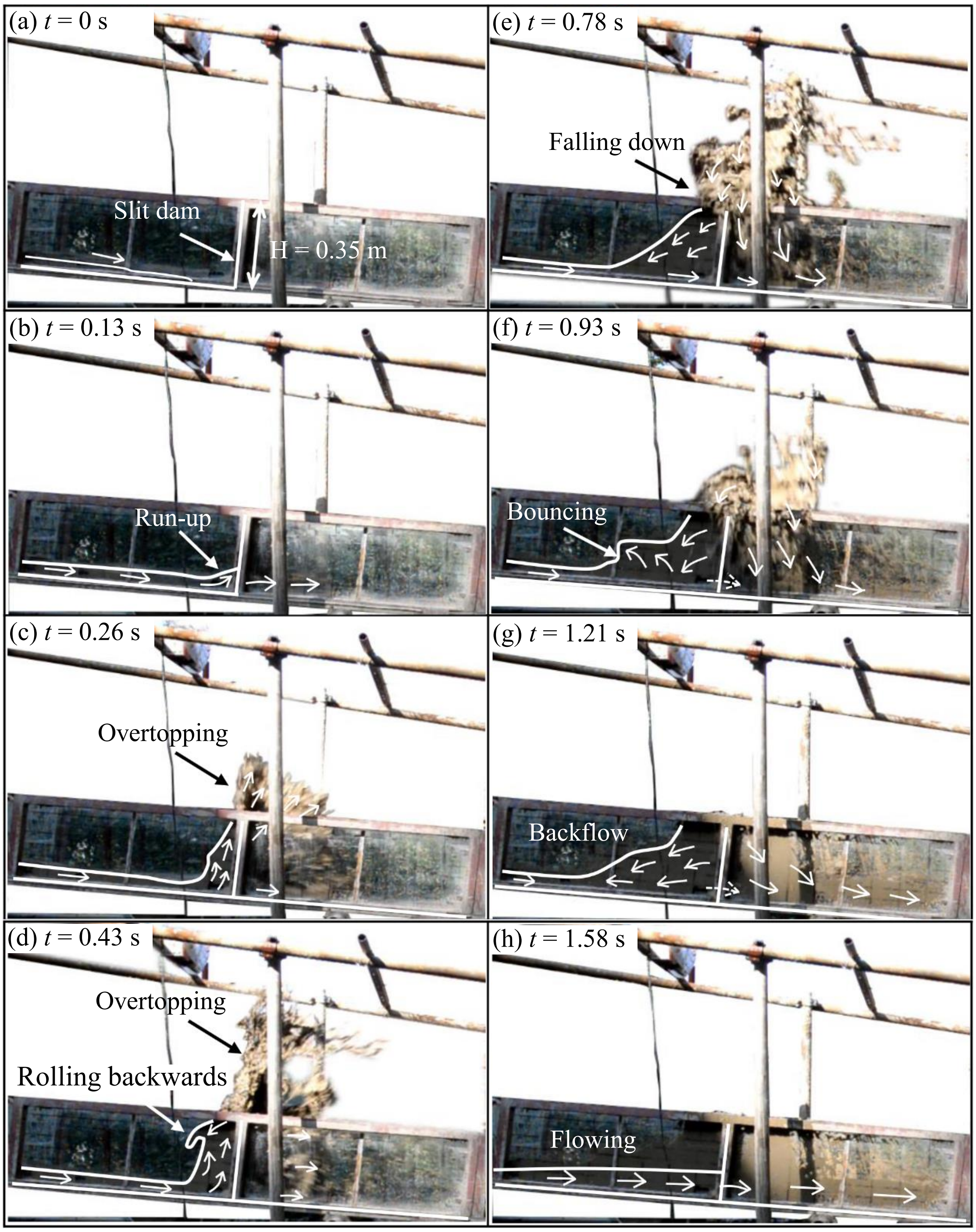


**Fig. 7** Interaction process between debris flow with high water content ($W$ = 30%) and slit dam with narrow relative post spacing ($b/d_{\max}$ = 1.4): test S-W30-1.4.


**Fig. 8** Interaction process between debris flow with high water content ($W$ = 30%) and slit dam with wide relative post spacing ($b/d_{max}$ = 3.1): test S-W30-3.1.

(a)

(b)

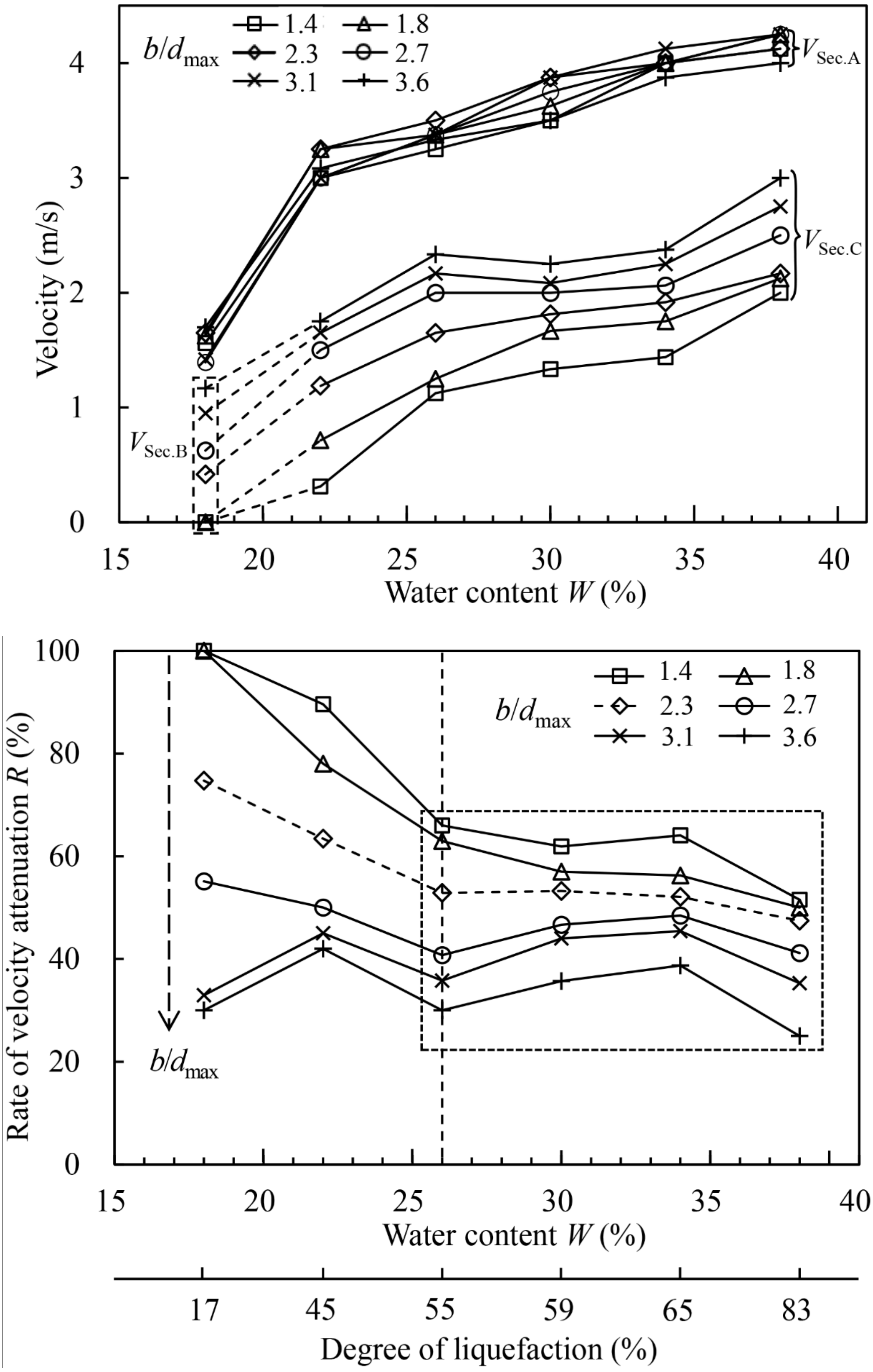


**Fig. 9** (a) relationship between velocity, water content, and relative post spacing $b/d_{max}$, velocity measured in Section B only for debris flow with water content of 18%; (b) rate of velocity attenuation $R$ with varying water content and relative post spacing $b/d_{max}$.

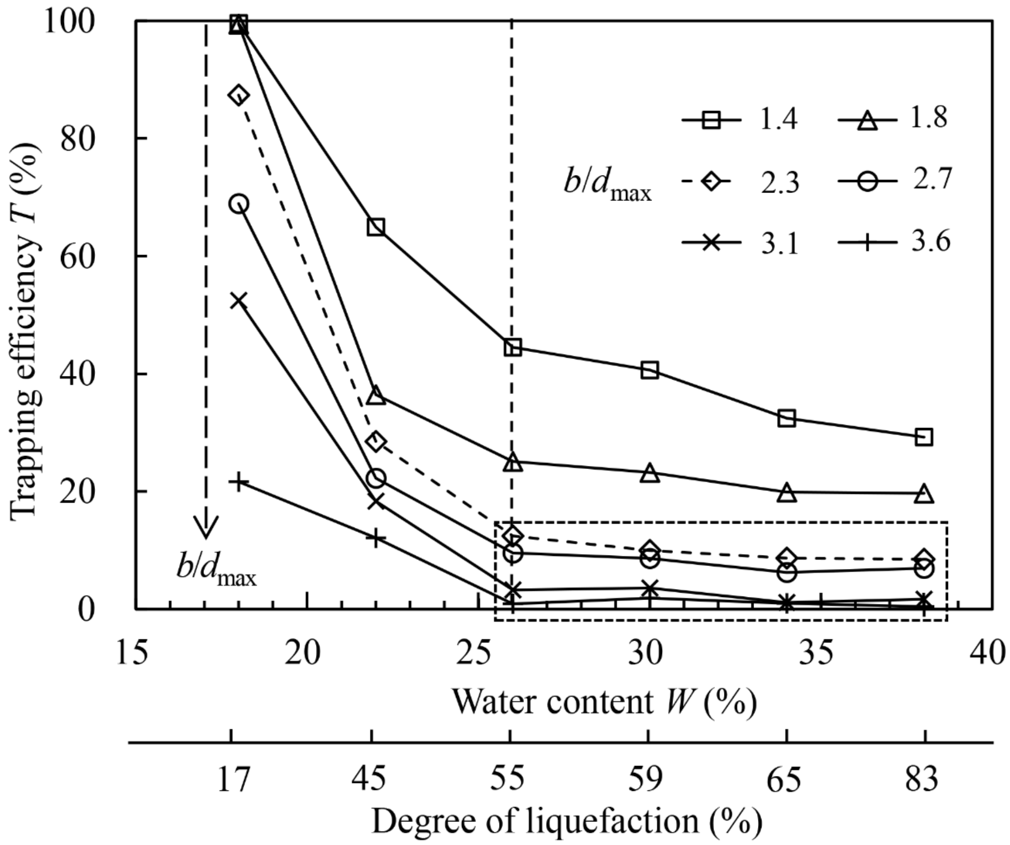


**Fig. 10** Trapping efficiency at varying water content and relative post spacing $b/d_{max}$.

(a)

(b)

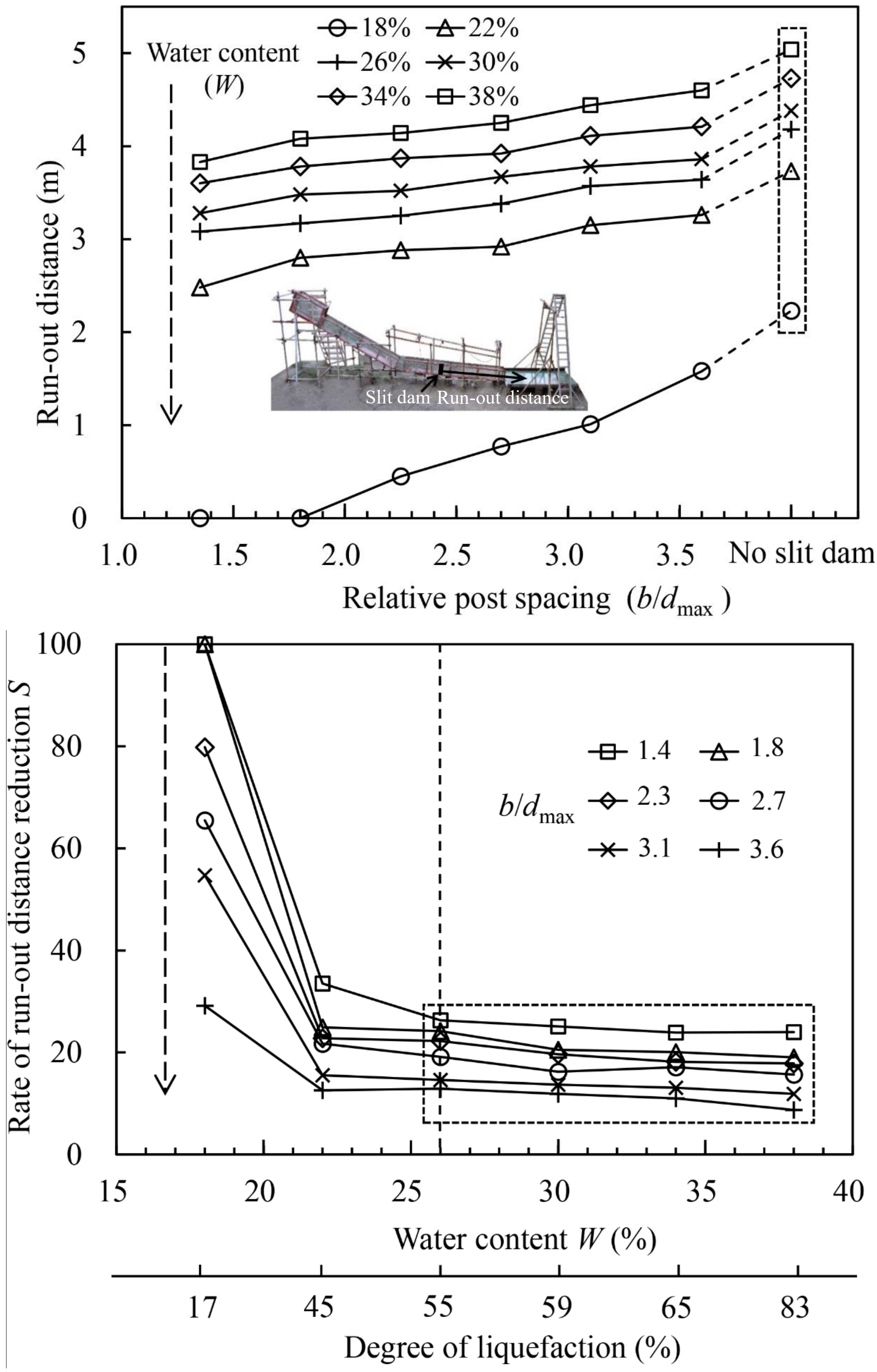


**Fig. 11** (a) run-out distance at varying water content and relative post spacing $b/d_{\max}$; (b) rate of run-out distance reduction $S$ at varying water content and relative post spacing $b/d_{\max}$.

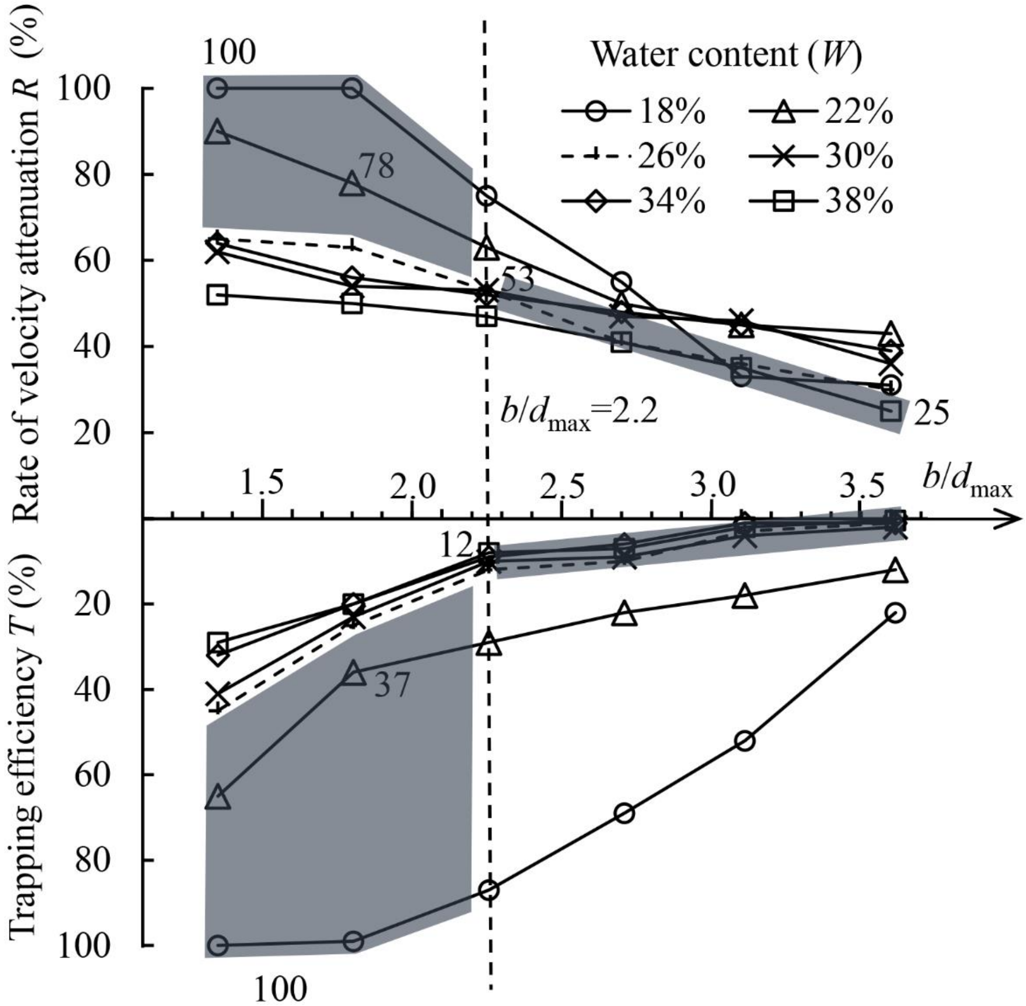


**Fig. 12** Comparison between rate of velocity attenuation $R$ and trapping efficiency $T$.

Table 1 Typical Froude numbers of natural debris flows

| Torrent | (Mean) Froude number *Fr* | Reference |
| --- | --- | --- |
| Illgraben catchment, Switzerland | 0.45~1.41 | McArdell *et al.* (2007) |
| Rio Reventado | 0.50 | Hübl *et al.* (2009) |
| Lesser Almatinka | 0.84 | |
| Wrightwood Canyon (1941) | 0.87 | |
| Wrightwood Canyon (1969) | 0.95 | |
| Bullock Greek | 1.26 | |
| Hunshui Gully | 1.90 | |
| Nojiri River | 2.71 | |
| Pine Creek | 7.56 | |
| Torrents in Hong Kong | ~3.00 | Kwan *et al.* (2015) |

**Table 2** Test program of debris flow-slit dam interaction

| Test ID | Relative post spacing $b/d_{max}$ | Water content $W$ (%) | Bulk density (kg/m³) | Solid concentration ($C_s$) | Degree of liquefaction $\sigma_w/\sigma_t$ | Approach velocity (m/s) | Flow depth (m) | Froude number $Fr$ |
|---|---|---|---|---|---|---|---|---|
| S-W18-1.4 | 1.4 | 18 | 2160 | 0.69 | 0.17 | 1.56 | 0.056 | 2.11 |
| S-W18-1.8 | 1.8 | | | | | 1.62 | 0.056 | 2.19 |
| S-W18-2.3 | 2.3 | | | | | 1.42 | 0.070 | 1.72 |
| S-W18-2.7 | 2.7 | | | | | 1.39 | 0.073 | 1.65 |
| S-W18-3.1 | 3.1 | | | | | 1.70 | 0.061 | 2.21 |
| S-W18-3.6 | 3.6 | | | | | 1.65 | 0.070 | 2.00 |
| R-W18 | No slit dam | | | | | 1.64 | 0.070 | 1.98 |
| S-W22-1.4 | 1.4 | 22 | 2010 | 0.63 | 0.45 | 3.00 | 0.045 | 4.53 |
| S-W22-1.8 | 1.8 | | | | | 3.25 | 0.035 | 5.57 |
| S-W22-2.3 | 2.3 | | | | | 3.25 | 0.035 | 5.57 |
| S-W22-2.7 | 2.7 | | | | | 3.00 | 0.039 | 4.87 |
| S-W22-3.1 | 3.1 | | | | | 3.00 | 0.040 | 4.81 |
| S-W22-3.6 | 3.6 | | | | | 3.08 | 0.043 | 4.76 |
| R-W22 | No slit dam | | | | | 3.00 | 0.044 | 4.59 |
| S-W26-1.4 | 1.4 | 26 | 1970 | 0.59 | 0.55 | 3.25 | 0.043 | 5.02 |
| S-W26-1.8 | 1.8 | | | | | 3.38 | 0.040 | 5.42 |
| S-W26-2.3 | 2.3 | | | | | 3.50 | 0.036 | 5.92 |
| S-W26-2.7 | 2.7 | | | | | 3.38 | 0.036 | 5.71 |
| S-W26-3.1 | 3.1 | | | | | 3.38 | 0.040 | 5.42 |
| S-W26-3.6 | 3.6 | | | | | 3.33 | 0.040 | 5.34 |
| R-W26 | No slit dam | | | | | 3.25 | 0.047 | 4.81 |
| S-W30-1.4 | 1.4 | 30 | 1920 | 0.56 | 0.59 | 3.50 | 0.049 | 5.07 |
| S-W30-1.8 | 1.8 | | | | | 3.62 | 0.050 | 5.19 |
| S-W30-2.3 | 2.3 | | | | | 3.88 | 0.044 | 5.93 |
| S-W30-2.7 | 2.7 | | | | | 3.75 | 0.041 | 5.94 |
| S-W30-3.1 | 3.1 | | | | | 3.88 | 0.040 | 6.22 |
| S-W30-3.6 | 3.6 | | | | | 3.50 | 0.046 | 5.23 |
| R-W30 | No slit dam | | | | | 3.75 | 0.038 | 6.17 |
| S-W34-1.4 | 1.4 | 34 | 1880 | 0.53 | 0.65 | 4.00 | 0.040 | 6.41 |
| S-W34-1.8 | 1.8 | | | | | 3.88 | 0.046 | 5.80 |
| S-W34-2.3 | 2.3 | | | | | 4.00 | 0.043 | 6.18 |
| S-W34-2.7 | 2.7 | | | | | 4.00 | 0.044 | 6.11 |
| S-W34-3.1 | 3.1 | | | | | 4.12 | 0.036 | 6.96 |
| S-W34-3.6 | 3.6 | | | | | 4.00 | 0.046 | 5.98 |
| R-W34 | No slit dam | | | | | 4.00 | 0.034 | 6.95 |
| S-W38-1.4 | 1.4 | 38 | 1830 | 0.50 | 0.83 | 4.12 | 0.049 | 5.97 |
| S-W38-1.8 | 1.8 | | | | | 4.25 | 0.045 | 6.42 |
| S-W38-2.3 | 2.3 | | | | | 4.12 | 0.036 | 6.96 |
| S-W38-2.7 | 2.7 | | | | | 4.25 | 0.039 | 6.90 |
| S-W38-3.1 | 3.1 | | | | | 4.25 | 0.042 | 6.65 |
| S-W38-3.6 | 3.6 | | | | | 4.00 | 0.043 | 6.18 |
| R-W38 | No slit dam | | | | | 4.08 | 0.040 | 6.54 |